Published in final edited form as:

Science. 2018 November 30; 362(6418): . doi:10.1126/science.aat0174.

Formyl-methionine as an N-degron of a eukaryotic N-end rule pathway

Jeong-Mok Kim[1], **Ok-Hee Seok**[1], **Shinyeong Ju**[2,3], **Ji-Eun Heo**[1], **Jeonghun Yeom**[2,4], **Da-Som Kim**[1], **Joo-Yeon Yoo**[1], **Alexander Varshavsky**[5], **Cheolju Lee**[2,4,6,*], and **Cheol-Sang Hwang**[1,*]

[1]Department of Life Sciences, Pohang University of Science and Technology, Pohang, Gyeongbuk 37673, Republic of Korea.

[2]Center for Theragnosis, Korea Institute of Science and Technology, Seoul 02792, Republic of Korea.

[3]Department of Life Science and Research Institute for Natural Sciences, Hanyang University, Seoul 04763, Republic of Korea.

[4]Division of Bio-Medical Science & Technology, KIST School, Korea University of Science and Technology, Seoul 02792, Republic of Korea.

[5]Division of Biology and Biological Engineering, California Institute of Technology, Pasadena, CA 91125, USA.

[6]Department of Converging Science and Technology, KHU-KIST, Kyung Hee University, Seoul 02447, Republic of Korea.

Abstract

In bacteria, nascent proteins bear the pretranslationally generated N-terminal (Nt) formyl-methionine (fMet) residue. Nt-fMet of bacterial proteins is a degradation signal, termed fMet/N-degron. By contrast, proteins synthesized by cytosolic ribosomes of eukaryotes were presumed to bear unformylated Nt-Met. Here we found that the yeast formyltransferase Fmt1, although imported into mitochondria, could also produce Nt-formylated proteins in the cytosol. Nt-formylated proteins were strongly up-regulated in stationary phase or upon starvation for specific amino acids. This up-regulation strictly required the Gcn2 kinase, which phosphorylates Fmt1 and mediates its retention in the cytosol. We also found that the Nt-fMet residues of Nt-formylated proteins act as fMet/N-degrons and identified the Psh1 ubiquitin ligase as the recognition component of the eukaryotic fMet/N-end rule pathway, which destroys Nt-formylated proteins.

[*]Corresponding author. cshwang@postech.ac.kr (C.-S.H.); clee270@kist.re.kr (C.L.).

Author contributions:

C.-S.H., J.-M.K., J.-Y.Y., C.L., A.V., and other coauthors designed the research. J.-M.K., O.-H.S., S.J., J.-E.H., J.Y., D.-S.K., and C.-S.H. performed the research, and all coauthors analyzed data. C.-S.H.,J.-M.K., C.L., and A.V. wrote the paper.

Competing interests:

All coauthors declare no competing interests.

Data and materials availability:

All mass spectrometric data of this study are available in the PRIDE database (accession number: PXD010780). All (other) data needed to evaluate the conclusions in the paper are present in the paper or in the supplementary materials.

SUPPLEMENTARY MATERIALS

www.sciencemag.org/content/362/6418/eaat0174/suppl/DC1

Graphical Abstract

INTRODUCTION: In both bacteria and eukaryotic mitochondria and chloroplasts, the ribosomal synthesis of proteins is initiated with the N-terminal (Nt) formyl-methionine (fMet) residue. Nt-fMet is produced pretranslationally by formyltransferases, which use 10-formyltetrahydrofolate as a cosubstrate. By contrast, proteins synthesized by cytosolic ribosomes of eukaryotes were always presumed to bear unformylated N-terminal Met (Nt-Met). The unformylated Nt-Met residue of eukaryotic proteins is often cotranslationally Ntacetylated, a modification that creates specific degradation signals, Ac/N-degrons, which are targeted by the Ac/N-end rule pathway. The N-end rule pathways are a set of proteolytic systems whose unifying feature is their ability to recognize proteins containing N-degrons, thereby causing the degradation of these proteins by the proteasome or autophagy in eukaryotes and by the proteasome-like ClpAP protease in bacteria. The main determinant of an N-degron is a destabilizing Nt-residue of a protein. Studies over the past three decades have shown that all 20 amino acids of the genetic code can act, in cognate sequence contexts, as destabilizing Nt-residues. The previously known eukaryotic N-end rule pathways are the Arg/N-end rule pathway, the Ac/N-end rule pathway, and the Pro/N-end rule pathway. Regulated degradation of proteins and their natural fragments by the N-end rule pathways has been shown to mediate a broad range of biological processes.

RATIONALE: The chemical similarity of the formyl and acetyl groups and their identical locations in, respectively, Nt-formylated and Nt-acetylated proteins led us to suggest, and later to show, that the Nt-fMet residues of nascent bacterial proteins can act as bacterial N-degrons, termed fMet/N-degrons. Here we wished to determine whether Nt-formylated proteins might also form in the cytosol of a eukaryote such as the yeast *Saccharomyces cerevisiae* and to determine the metabolic fates of Nt-formylated proteins if they could be produced outside mitochondria. Our approaches included molecular genetic techniques, mass spectrometric analyses of proteins' N termini, and affinity-purified antibodies that selectively recognized Nt-formylated reporter proteins.

RESULTS: We discovered that the yeast formyltransferase Fmt1, which is imported from the cytosol into the mitochondria inner matrix, can generate Nt-formylated proteins in the cytosol, because the translocation of Fmt1 into mitochondria is not as efficacious, even under unstressful conditions, as had previously been assumed. We also found that Nt-formylated proteins are greatly up-regulated in stationary phase or upon starvation for specific amino acids. The massive increase of Nt-formylated proteins strictly requires the Gcn2 kinase, which phosphorylates Fmt1 and mediates its retention in the cytosol. Notably, the ability of Gcn2 to retain a large fraction of Fmt1 in the cytosol of nutritionally stressed cells is confined to Fmt1, inasmuch as the Gcn2 kinase does not have such an effect, under the same conditions, on other examined nuclear DNA–encoded mitochondrial matrix proteins. The Gcn2-Fmt1 protein localization circuit is a previously unknown signal transduction pathway. A down-regulation of cytosolic Nt-formylation was found to increase the sensitivity of cells to undernutrition stresses, to a prolonged cold stress, and to a toxic compound. We also discovered that the Nt-fMet residues of Nt-formylated cytosolic proteins act as eukaryotic fMet/N-degrons and identified the Psh1 E3 ubiquitin ligase as the recognition component (fMet/N-recognin) of the previously unknown eukaryotic fMet/N-end rule pathway, which destroys Nt-formylated proteins.

CONCLUSION: The Nt-formylation of proteins, a long-known pretranslational protein modification, is mediated by formyltransferases. Nt-formylation was thought to be confined to bacteria and bacteria-descended eukaryotic organelles but was found here to also occur at the start of translation by the cytosolic ribosomes of a eukaryote. The levels of Nt-formylated eukaryotic proteins are greatly increased upon specific stresses, including undernutrition, and appear to be important for adaptation to these stresses. We also discovered that Nt-formylated cytosolic proteins are selectively destroyed by the eukaryotic fMet/N-end rule pathway, mediated by the Psh1 E3 ubiquitin ligase. This previously unknown proteolytic system is likely to be universal among eukaryotes, given strongly conserved mechanisms that mediate Nt-formylation and degron recognition.

—The eukaryotic fMet/N-end rule pathway.

(Top) Under undernutrition conditions, the Gcn2 kinase augments the cytosolic localization of the Fmt1 formyltransferase, and possibly also its enzymatic activity. Consequently, Fmt1 up-regulates the cytosolic fMet–tRNAi (initiator transfer RNA), and thereby increases the levels of cytosolic Nt-formylated proteins, which are required for the adaptation of cells to specific stressors. (Bottom) The Psh1 E3 ubiquitin ligase targets the N-terminal fMet-residues of eukaryotic cytosolic proteins, such as Cse4, Pgd1, and Rps22a, for the polyubiquitylation-mediated, protea-some-dependent degradation.

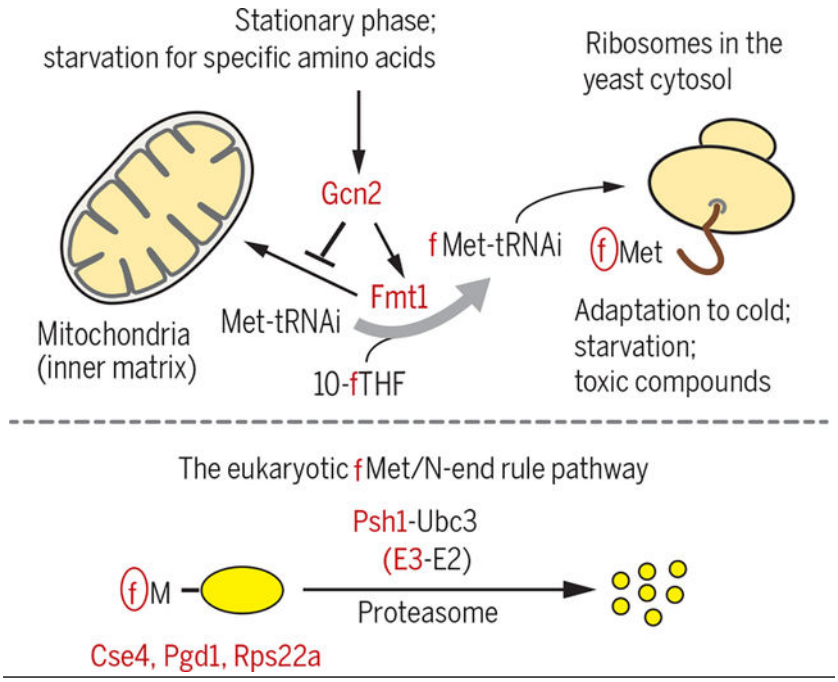

Nascent proteins bear the N-terminal (Nt) methionine residue, encoded by the AUG initiation codon. In bacteria and in eukaryotic mitochondria and chloroplasts, virtually all nascent proteins bear the N-terminal formyl-methionine (Nt-fMet), which is generated pretranslationally. Formyltransferases (FMTs) use 10-formyltetrahydrofolate as a cosubstrate to N^{α}-terminally formylate the Met moiety of initiator Met-tRNAs. Consequently, nascent bacterial proteins bear Nt-fMet (1–7). By contrast, proteins synthesized by the cytosolic ribosomes of eukaryotes bear the unformylated Nt-Met residue.

This Nt-Met is often N^{α}-terminally acetylated by Nt-acetylases (8). We have previously shown that the cotranslational Nt-acetylation of eukaryotic proteins creates specific degradation signals, termed Ac/N-degrons, that are targeted by a distinct N-end rule pathway, termed the Ac/N-end rule pathway (fig. S1F) (9–13).

The N-end rule pathways are a set of proteolytic systems whose unifying feature is their ability to recognize proteins containing degradation signals called N-degrons, thereby causing the degradation of these proteins by the proteasome or autophagy in eukaryotes and by the proteasome-like ClpAP protease in bacteria (fig. S1) (9–26). The main determinant of an N-degron is a destabilizing Nt-residue of a protein. Initially, most N-degrons are pro–N-degrons. They are converted to active N-degrons either constitutively (e.g., during the emergence of a protein from a ribosome) or conditionally, via regulated steps. Among the routes to N-degrons are site-specific cleavages of proteins by proteases such as, for example, caspases or calpains, and/or enzymatic Nt-acetylation, Nt-deamidation, Nt-arginylation, or Nt-leucylation of specific proteins at the α-amino groups of their Nt-residues (10, 22). Studies over the past three decades have shown that all 20 amino acids of the genetic code can act, in cognate sequence contexts, as destabilizing Nt-residues (fig. S1). Consequently, many proteins in a cell are conditionally short-lived N-end rule substrates, either as full-length proteins or as protease-generated natural protein fragments. Recognition components of N-end rule pathways, called N-recognins, are either E3 ubiquitin (Ub) ligases or other proteins that can target N-degrons (10, 22).

Regulated degradation of proteins and/or their fragments by the N-end rule pathways mediates a multitude of processes, including the sensing of oxygen, nitric oxide, and heme; the control of subunit stoichiometries in protein complexes; the elimination of misfolded proteins and also of proteins retrotranslocated to the cytosol from other compartments; the regulation of apoptosis and repression of neurodegeneration; the regulation of DNA repair, transcription, replication, and chromosome cohesion and segregation; the regulation of chaperones, G proteins, cytoskeletal proteins, autophagy, gluconeogenesis, peptide import, meiosis, circadian rhythms, fat metabolism, cell migration, immunity, cardiovascular development, spermatogenesis, and neurogenesis; and the regulation of leaf development, senescence, and many other processes in plants [(10, 18–20, 22) and references therein].

Eukaryotes have been known to contain three N-end rule pathways. One of them is the Ac/N-end rule pathway (fig. S1F) (9–13). At least 60 and 80% of nascent proteins in, respectively, the yeast *Saccharomyces cerevisiae* and human cells are cotranslationally and irreversibly Nt-acetylated by ribosome-associated Nt-acetylases (8). Many Nt-acetylated proteins contain Ac/N-degrons, whose regulation includes their reversible steric shielding in cognate protein complexes (11–13, 27).

Another N-end rule pathway is the Arg/N-end rule pathway. It targets unacetylated Nt-residues (fig. S1G) (10, 14, 15, 28). N-terminal Arg, Lys, His, Leu, Phe, Tyr, Trp, Ile, and Met (if Met is followed by a bulky hydrophobic residue) are directly recognized by N-recognins (12, 29, 30). By contrast, N-terminal Asn, Gln, Glu, and Asp (as well as Cys, under some conditions) are destabilizing owing to enzymatic deamidation of Nt-Asn and Nt-Gln and Nt-arginylation of Nt-Asp and Nt-Glu (25, 26, 31).

The third eukaryotic N-end rule pathway, termed the Pro/N-end rule pathway, targets proteins that bear the Nt-Pro residue or a Pro at position two, in addition to adjoining and required sequence motifs (fig. S1E) (20). Physiological substrates of the Pro/N-end rule pathway include gluconeogenic enzymes, which are long-lived in cells deprived of glucose but are selectively destroyed upon return to glucose-replete conditions (20).

N-terminally formylated proteins in eukaryotic cytosol

In bacteria, the formyl group of Nt-fMet is cotranslationally removed from most (though not all) nascent proteins by the ribosome-associated peptide-deformylase (PDF) (2, 3, 5). Some fungal and animal genomes, such as those of *S. cerevisiae* and the nematode *Caenorhabditis elegans*, do not encode proteins that are sequelogous [similar in sequence (32)] to PDFs (6). By contrast, the FMTs, which produce fMet-tRNAi from Met-tRNAi are encoded by all examined eukaryotic genomes, in addition to being universal among bacteria. Mitochondrial FMTs, specified by nuclear DNA, are imported from the cytosol to the inner matrix of mitochondria. Consequently, eight proteins that are encoded by the *S. cerevisiae* mitochondrial DNA, are pretranslationally Nt-formylated at the start of their synthesis in the matrix and retain the formyl group of their Nt-fMet, in agreement with the (inferred) absence of PDF in yeast (6).

Nt-acetylation of eukaryotic proteins creates Ac/N-degrons (fig. S1F) (9–13). The chemical similarity of the formyl and acetyl groups and their identical locations in, respectively, Nt-formylated and Nt-acetylated proteins led us to suggest (9), and later to show (7), that the fMet residues at the N termini of nascent bacterial proteins can act as bacterial N-degrons, termed fMet/N-degrons (fig. S1C).

Given this function of Nt-fMet in bacteria (7), and also because a eukaryotic FMT enzyme, before its import into mitochondria, is transiently cytosolic, we began this study by expressing *Escherichia coli* FMT (*Ec*FMT) in yeast. Such an expression was previously shown to convert up to 70% of yeast Met-tRNAi to fMet-tRNAi and to inhibit growth, suggesting that Nt-formylated proteins might be generated in the yeast cytosol (4). Our initial aim was to address this possibility directly and to determine the metabolic fate of Nt-formylated proteins if they could be produced outside mitochondria.

*Ec*FMT or vector alone were expressed in yeast from the P_{GAL1} promoter. Wild-type *Ec*FMT (but not its inactive *Ec*FMT^{R43L} mutant; R43L, Arg^{43}→Leu) retarded yeast growth (fig. S2B). These assays involved stable-isotope labeling by amino acids in cell culture (SILAC), an enrichment for Nt-peptides, and capillary liquid chromatography–tandem mass spectrometry (cLC-MS/MS) (fig. S2A). We found that ~11% of nuclear DNA–encoded proteins that yielded Nt-peptides analyzable by cLC-MS/MS were Nt-formylated in yeast cells that expressed *Ec*FMT. Forty-two Nt-formylated peptides were detected by cLC-MS/MS, out of 467 distinct Nt-peptides, which were derived from 357 detected proteins (fig. S2, A, C, and E, and table S1).

An unexpected result of these analyses was the outcome of controls: In yeast lacking *Ec*FMT, ~3% of nuclear DNA–encoded nonmitochondrial proteins contained Nt-fMet (figs.

S2, A, C, and D, and S3; and table S1). Thus, notably, proteins containing Nt-fMet were synthesized in the yeast cytosol under normal conditions as well. Additional and independent evidence for this conclusion is described below.

Nt-formylated proteins in wild-type (lacking *Ec*FMT) yeast that were identified by cLC-MS/MS were Act1 (actin), Bos1 (a SNAP receptor), Bud27 (a bud site selector), Rps28a and Rps28b (ribosomal proteins), Leu2 (3-isopropyl malate dehydrogenase), Sup45 (a peptide chain release factor), Dyn2 (a dynein light chain), Uso1 (a vesicle transporter), and Vps52 (a vacuolar sorting–associated protein) (figs. S2D and S3). We also detected mitochondrial DNA–encoded Cox3, which is produced by mitochondrial ribosomes and thus would be expected to bear Nt-fMet, in contrast to nuclear DNA–encoded proteins (figs. S2D and S3G) (6).

A parsimonious explanation of these results is that Nt-formylation of nonmitochondrial proteins in wild-type (lacking *Ec*FMT) yeast is caused by low but notable cytosolic levels of the nuclear DNA–encoded *S. cerevisiae* Fmt1 (*Sc*Fmt1) formyltransferase. In this interpretation, the translocation of *Sc*Fmt1 from the cytosol (in which *Sc*Fmt1 is produced) into the mitochondrial matrix (in which *Sc*Fmt1 normally resides) is not as efficient, even under unstressful conditions, as had previously been assumed. Consequently, enough *Sc*Fmt1 would be present in the cytosol to cause the formation of cytosolic fMet-tRNAi and the pretranslational Nt-formylation of cytosolic proteins (fig. S2D and tables S1 and S2). This explanation was found to be correct—the levels of an Nt-formylated Nt-fMet reporter became negligible in *fmt1*Δ yeast (Fig. 1, B and D; see below for details).

Given the pretranslational synthesis of fMet-tRNA, one would expect, a priori, a uniform “partitioning” of the Nt-fMet residues among all or most proteins of a cell’s proteome. We do not understand why the actual mass spectrometry (MS)–based results (figs. S2, D and E, and S3; and tables S1 and S2) are different from this expectation, that is, why only some proteins were detected as (partially) Nt-formylated ones. Plausible explanations include an incomplete cLC-MS/MS–mediated coverage of the proteome, different rates of degradation of specific Nt-formylated proteins, and/or that the efficiency of translation initiation with fMet-tRNAi is not the same for all proteins synthesized in the cytosol.

Antibody to N-terminally formylated protein reporters

The 33-kDa reporter, denoted as MD-D2-e^{K}-ha-GST, was identical to our previously characterized reporter MD-D2-e^{K}-ha-Ura3, save for the glutathione transferase (GST) moiety, used alternately with Ura3 (7). The reporter comprised the Nt-sequence MDIAIGTYQEK [denoted as MD-D2 (7)], followed by a 44-residue sequence e^{K} [extension (e) containing lysine (K)], by the ha epitope (YPYDVPDYA), by the AFLGQ linker (9), and by either GST or Ura3 (Figs. 1A and 2B). The e^{K} segment is often used in reporters because it is unstructured (disordered) while lacking degrons in *E. coli* and yeast (10). MD-D2-GST was identical to MD-D2-e^{K}-ha-GST save for the absence of the e^{K}-ha segment (Fig. 1B). (Single-letter abbreviations for amino acid residues are as follows: A, Ala; C, Cys; D, Asp; E, Glu; F, Phe; G, Gly; H, His; I, Ile; K, Lys; L, Leu; M, Met; N, Asn; P, Pro; Q, Gln; R, Arg; S, Ser; T, Thr; V, Val; W, Trp; and Y, Tyr.)

Cycloheximide (CHX)–chases with MD-D2-e^{K}-ha-Ura3 or MD-D2-e^{K}-ha-GST showed that these reporters were short-lived in wild-type *S. cerevisiae* but were nearly completely stable in double-mutant *naa20*Δ *ubr1*Δ cells that lacked both the NatB (Naa20) Nt-acetylase and the Arg/N-end rule pathway (owing to the absence of Ubr1) (fig. S4, A and B). The *naa20*Δ mutation abrogated the otherwise expected Nt-acetylation, by NatB, of MD-D2-e^{K}-ha–based reporters and thereby precluded their degradation by the Ac/N-end rule pathway (8–13). Given the stability of MD-D2-e^{K}-ha–based reporters in *naa20*Δ *ubr1*Δ cells (fig. S4, A and B), most degradation assays were performed in this genetic background.

To detect Nt-fMet by a method independent of mass spectrometry, the synthetic Nt-formylated peptide fMDIAIGTYQEK (the fMD-D2 moiety; Fig. 1, A and B) was used to produce an affinity-purified rabbit antibody, termed anti–MD-D2^{fM}, which recognized the above Nt-formylated peptide and also fMD-D2-GST but did not recognize their unformylated or Nt-acetylated counterparts (Fig. 1E). Nt-formylated and unformylated MD-D2-GST were produced in *E. coli* that were either incubated or not incubated with actinonin, an inhibitor of PDF-mediated deformylation (5). The presence of Nt-fMet or unformylated Nt-Met in MD-D2-GST was verified using both MS and anti–MD-D2^{fM} antibody (Fig. 1F and fig. S5).

SDS–polyacrylamide gel electrophoresis (SDS-PAGE) and immunoblotting with anti–MD-D2^{fM} detected Nt-formylated fMD-D2-GST in extracts from *Ec*FMT-expressing yeast (Fig. 1, B and G). More sensitive immunoprecipitation-immunoblotting assays could also detect fMD-D2-GST in extracts from yeast that lacked *Ec*FMT (Fig. 1D). The specificity of anti–MD-D2^{fM} (Fig. 1, E and F) was also confirmed by observing the quenching of immunoblotting signal by the Nt-formylated fMD-D2 peptide but not by its unformylated counterpart (Fig. 1G).

In cells expressing MD-D2-GST, the Nt-fMet residue of fMD-D2-GST was generated pretranslationally (see introduction) (Fig. 1B). By contrast, MD-D2-GST was generated cotranslationally from Ub-MD-D2-GST (bearing the Nt-Ub moiety) upon the cleavage-mediated removal of Nt-Ub by deubiquitylases (Fig. 1C) (10). Whereas directly expressed MD-D2-GST could be readily detected (using anti–MD-D2^{fM}) as the Nt-formylated fMD-D2-GST species, no Nt-fMet was detected in MD-D2-GST* that resulted from deubiquitylation of Ub-MD-D2-GST (the asterisk of MD-D2-GST* denotes its distinct origin) (Fig. 1, C and G). Besides confirming the specificity of anti–MD-D2^{fM}, these results indicated the pre-translational (at the level of fMet-tRNAi) origin of the Nt-fMet moiety of fMD-D2-GST. In addition, coexpression of *Ec*FMT and *E. coli* PDF (*Ec*PDF) (but not of its inactive mutant) in yeast strongly down-regulated the Nt-formylated fMD-D2-GST (Fig. 1G), in agreement with the (inferred) absence of PDF in *S. cerevisiae* (6).

Selective degradation of Nt-formylated proteins

The expression of *Ec*FMT in yeast resulted in rapid degradation of the otherwise long-lived MD-D2-e^{K}-ha-Ura3 and MD-D2-e^{K}-ha-GST (Fig. 2, A to D, and fig. S4, E to I). By contrast, no discernible degradation of MD-D2-e^{K}-ha-Ura3 or MD-D2-e^{K}-ha-GST occurred upon expression of the inactive *Ec*FMT^{R43L} mutant or vector alone (Fig. 2, C and D, and fig.

S4, E, F, and H). The *Ec*FMT-induced degradation of MD-D2-e^{K}-ha-GST and MD-D2-e^{K}-ha-Ura3 in yeast was nearly abolished by coexpression of the *Ec*PDF but not of its inactive *Ec*PDF^{E134A} mutant (Fig. 2, B and E, and fig. S4G).

Increasing the levels of *Ec*FMT, using the incrementally stronger yeast promoters P$_{ADH1}$, P$_{TEF1}$, and P$_{TDH3}$, progressively destabilized MD-D2-e^{K}-ha-GST, in part by decreasing its prechase (time-zero) levels (fig. S4H). By contrast, the expression of inactive *Ec*FMT^{R43L} had no effect (fig. S4H). *Ec*FMT did not discernibly alter the rate of protein synthesis in *S. cerevisiae*, in comparison to expression of inactive *Ec*FMT^{R43L} (fig. S6, A and B).

Tandem Ub-binding entity (TUBE)–pulldowns showed that MD-D2-e^{K}-ha-GST was polyubiquitylated in yeast upon expression of *Ec*FMT (but not of inactive *Ec*FMT^{R43L}), suggesting that the degradation of Nt-formylated fMD-D2-e^{K}-ha-GST was Ub-dependent (Fig. 2F). Assays with MG132, a proteasome inhibitor, indicated that the degradation of fMD-D2-e^{K}-ha-GST was also proteasome-dependent (fig. S4I). Importantly, the use of anti–MD-D2^{fM} showed that the *Ec*FMT-induced degradation of MD-D2-e^{K}-ha–based fusions involved, selectively, their Nt-formylated subsets (fig. S4I).

Together, these results (Figs. 1 and 2, and figs. S2 and S4) indicated that the *Ec*FMT-mediated production of fMet-tRNAi in the yeast cytosol causes the synthesis of Nt-formylated proteins, which are rapidly degraded. This degradation required the Nt-fMet residue of an Nt-formylated protein because the protein could be stabilized by coexpression of the active (but not inactive) *Ec*PDF (Fig. 2E and fig. S4G).

We conclude that the Nt-fMet residues of proteins in a eukaryotic cell could act as specific degradation signals, termed fMet/N-degrons. The bulk of these results were obtained with *S. cerevisiae* that ectopically expressed *Ec*FMT. Crucially, however, a minor, but discernible, fraction of nuclear DNA–encoded nonmitochondrial yeast proteins contained Nt-fMet even in *S. cerevisiae* that did not express *Ec*FMT (figs. S2D and S3, and tables S1 and S2).

Degradation of Nt-formylated proteins requires the Psh1 E3 ubiquitin ligase

Given these results, we screened a collection of single-mutant *S. cerevisiae* strains that lacked specific E3 Ub ligases and expressed both *Ec*FMT and MD-D2-e^{K}-ha-GST. (*Ec*FMT was used to augment the synthesis of Nt-formylated proteins.) Extracts from 78 mutant strains were fractionated by SDS-PAGE and immunoblotted with anti-ha, anti–MD-D2^{fM}, and anti-tubulin (fig. S7). Anti-ha detected all species of MD-D2-e^{K}-ha-GST, whereas anti–MD-D2^{fM} selectively detected fMD-D2-e^{K}-ha-GST. The Nt-formylated fMD-D2-e^{K}-ha-GST (relative to total MD-D2-e^{K}-ha-GST) was strongly increased in the *psh1*Δ mutant, implying the in vivo stabilization of fMD-D2-e^{K}-ha-GST in the absence of Psh1 (fig. S7A, lane 10).

Nt-formylated fMD-D2-e^{K}-ha-GST was also increased in three other E3 mutants (figs. S7A, lane 13; S7D, lane 9; and S7F, lane 11). However, those increases were much less than the one in *psh1*Δ cells and were also accompanied by higher levels of total MD-D2-e^{K}-ha-GST, in contrast to the strong and selective increase of fMD-D2-e^{K}-ha-GST in *psh1*Δ cells (fig. S7A, lane 10). In agreement with this screen (fig. S7), the degradation of fMD-D2-e^{K}-ha-

GST required the Psh1 E3 (Fig. 3A). In addition, the polyubiquitylation of MD-D2-e^K-ha-GST was nearly abolished in *psh1*Δ yeast, despite the presence of *Ec*FMT (Fig. 2F, lane 4).

The levels of mRNA encoding MD-D2-e^K-ha-GST were approximately equal in *PSH1* versus *psh1*Δ yeast (fig. S8A). Furthermore, C-terminally flag-tagged Psh1 ($Psh1_f$) interacted with the Nt-formylated fMD-D2-GST but not with its unformylated counterpart, indicating that physical binding by the Psh1 E3 required the Nt-formyl group of fMD-D2-GST (Fig. 3B).

We conclude that Psh1 is an N-recognin, termed the fMet/N-recognin, of a eukaryotic N-end rule pathway, termed the fMet/N-end rule pathway (fig. S1B). Psh1 is a 406-residue RING-type E3 Ub ligase that acts together with the Ubc8 or Ubc3 E2 enzymes (33–36). In *Ec*FMT-expressing yeast, the degradation of fMD-D2-e^K-ha-GST was comparably efficacious in *UBC8* and *ubc8*Δ cells (fig. S8C). By contrast, fMD-D2-e^K-ha-GST was stabilized in a temperature-sensitive Ubc3 ($Ubc3^{ts}$) mutant at nonpermissive temperature, indicating that the Psh1 fMet/N-recognin mediates the fMet/N-end rule pathway largely together with the Ubc3 E2 (figs. S1B and S8B).

Nt-formylation of the Cse4 histone accelerates its Psh1-mediated degradation

Until now, the sole known physiological substrate of Psh1 was Cse4 (called CENP-A in mammals), the centromere-specific histone H3 variant whose degradation is both Psh1-dependent and proteasome-dependent (33–37). Using the same approach that yielded anti–MD-$D2^{fM}$, we produced an antibody, termed anti-$Cse4^{fM}$, that selectively recognized the Nt-formylated fMet-Cse4 (fig. S4, C and D). C-terminally ha-tagged Cse4 ($Cse4_{ha}$) was strongly destabilized, in a Psh1-dependent manner, in wild-type yeast that expressed *Ec*FMT (but not its inactive *Ec*FMT^{R43L} mutant) (Fig. 3, C and D, and fig. S8H).

Recognition of Cse4 by Psh1 involves the CENP-A targeting domain (CATD) of Cse4 (Fig. 3C) (34, 35). To address the targeting of Cse4 through its Nt-fMet residue versus the CATD, we replaced CATD with the loop 1–α2 helix of the histone fold domain (HFD) of the main histone H3 (34), yielding a chimeric $Cse4^{HFD}_{ha}$ protein. In the absence of *Ec*FMT, $Cse4^{HFD}_{ha}$ was longer-lived than $Cse4_{ha}$, but both $Cse4^{HFD}_{ha}$ and $Cse4_{ha}$ were strongly destabilized in yeast that expressed the active (but not inactive) *Ec*FMT (Fig. 3, C and D, and fig. S8E). Immunoblotting with anti-$Cse4^{fM}$ confirmed the Nt-formylation of $Cse4^{HFD}_{ha}$ in the presence of *Ec*FMT (fig. S4D). In agreement with these results, $Cse4^{HFD}_{ha}$, which was short-lived in *Ec*FMT-expressing wild-type yeast, was stabilized either by coexpression of the *Ec*PDF or by ablation of the yeast Psh1 E3 (Fig. 3, D and E, and fig. S8E). $Cse4^{HFD}_{ha}$ was also stabilized in yeast $Ubc3^{ts}$ cells (but not in *ubc8*Δ cells) at nonpermissive temperature, again indicating that Ubc3 is the main E2 of the Psh1-mediated fMet/N-end rule pathway (fig. S8, E and F).

Psh1-mediated targeting of fMet/N-degrons in proteins other than Cse4

Thus far, 42 yeast proteins have been identified, by cLC-MS/MS, as those that are partially Nt-formylated in *Ec*FMT-expressing *S. cerevisiae* (fig. S2E). We asked whether some of these proteins were metabolically unstable, and, if so, whether the bulk of their degradation required both Nt-formylation and the Psh1 Ub ligase.

Forty-one proteins (all except Leu2) (fig. S2E) were C-terminally ha tagged and analyzed by CHX-chases in *PSH*1 and *psh1*Δ yeast cells that expressed *Ec*FMT. Anti-ha cannot distinguish between Nt-formylated and unformylated versions of these proteins. Observing the degradation of a protein that was dependent on both the Psh1 E3 and *Ec*FMT would indicate that a large fraction of the protein's molecules contained Nt-fMet. Out of 41 proteins examined, these assays identified two proteins, Pgd1 and Rps22a, whose degradation required both Psh1 and *Ec*FMT (fig. S6, C to H), similarly to the Cse4 histone (Fig. 3, C to E, and fig. S8, E to H).

Pgd1 is a subunit of the Mediator complex that functions together with RNA polymerase II (38). Degradation of Pgd1 required both *Ec*FMT and the Psh1 E3 and could be counteracted by coexpression of the *Ec*PDF (but not of its inactive mutant) (fig. S6D). Similar results were obtained with the ribosomal protein Rps22a (fig. S6H). The other 39 proteins, which were also partially Nt-formylated in *Ec*FMT-expressing yeast (fig. S2E), yielded negative results (an example, with Hxk1, is shown in fig. S6I).

Thus, although Nt-formylated versions of the above proteins in *Ec*FMT-expressing yeast could be detected by cLC-MS/MS (fig. S2E), the relative levels of Nt-formylated proteins, vis-à-vis their unformylated counterparts, would be too low for observing degradation of Nt-formylated species using anti-ha, which did not distinguish between Nt-formylated and unformylated versions of these proteins. Another, not mutually exclusive explanation would be the conditionality of fMet/N-degrons in these endogenous (not overexpressed) proteins, owing to a rapid posttranslational shielding (sequestration) of their fMet/N-degrons. The shielding would occur through an intramolecular protein folding and/or through formation of oligomeric protein complexes. This mechanism of conditionality has been demonstrated for Ac/N-degrons in proteins whose degradation by the Ac/N-end rule pathway could be halted in the presence of their natural protein ligands (11).

Psh1-mediated destruction of Nt-formylated proteins counteracts their toxicity

Slow growth of *Ec*FMT-expressing *S. cerevisiae* could be rescued by expression of *Ec*PDF but not of its inactive mutant (4). Because the levels of Nt-formylated proteins are increased in *Ec*FMT-expressing yeast (Fig. 1G; fig. S2, C to E; and table S1), and because the Psh1 Ub ligase mediates the degradation of Nt-formylated proteins (Fig. 3, A, B, and D; and figs. S6, C, E, and F, and S8, E, G, and H), an ablation of Psh1 would be expected to make cells hypersensitive to Nt-formylated proteins. In agreement with this prediction, the growth defect of *Ec*FMT-expressing yeast was notably higher in *psh1*Δ cells, either on plates or in liquid cultures (fig. S9). Deformylation of Nt-formylated proteins, through a coexpression of

*Ec*PDF (but not of its inactive mutant), nearly abolished the growth-rate difference between *PSH1* and *psh1*Δ cells that expressed *Ec*FMT (fig. S9B).

These (fig. S9) and other results (see below) implied an increase in steady-state levels of Nt-formylated proteins both in *psh1*Δ cells and in stationary-phase wild-type cells. We performed additional SILAC-based cLC-MS/MS surveys (as described above and in fig. S2), but this time without ectopic *Ec*FMT, and with stationary-phase wild-type cells versus stationary-phase *psh1*Δ cells. This set of MS/MS analyses, with cells not expressing *Ec*FMT, identified 21 Nt-formylated proteins in wild-type yeast and 26 Nt-formylated proteins in *psh1*Δ yeast, with both cultures in stationary phase (table S2).

Up-regulation of Nt-formylated proteins upon starvation for specific amino acids

Similarly to the effect of expressing *Ec*FMT in *S. cerevisiae*, an expression, also in yeast, of *Sc*Fmt1$^{\Delta 1-26}$, a derivative of the yeast *Sc*Fmt1 that lacked its mitochondrial presequence, increased the levels of Nt-formylated fMD-D2-GST (fig. S8D). The levels of Nt-formylated fMD-D2-GST were further increased when yeast cultures expressing *Sc*Fmt1$^{\Delta 1-26}$ reached the stationary phase, despite the presence of the fMet/N-end rule pathway in these cells (Fig. 4A and fig. S1B).

A strong increase of Nt-formylated fMD-D2-GST was also observed with wild-type stationary-phase yeast, that is, with cells that expressed neither *Ec*FMT nor the presequence-lacking *Sc*Fmt1$^{\Delta 1-26}$ (Fig. 4B). By contrast, no Nt-formylated fMD-D2-GST was present in *fmt1*Δ yeast under any growth conditions (Figs. 1D and 4B). These results were an independent confirmation of the cLC-MS/MS findings that the endogenous wild-type *Sc*Fmt1, though normally imported into mitochondria, also mediated the synthesis of Nt-formylated cytosolic proteins (fig. S2D and tables S1 and S2).

We wished to identify other stresses, more specific than stationary phase, that could up-regulate Nt-formylated proteins. To facilitate the detection of Nt-formylated fMD-D2-GST by anti–MD-D2^{fM}, wild-type *Sc*Fmt1 was moderately over-expressed from a low-copy plasmid and the constitutive P_{TDH3} promoter in *psh1*Δ *S. cerevisiae*, which lacked the fMet/N-end rule pathway and could not degrade Nt-formylated proteins.

Nt-formylated fMD-D2-GST was greatly up-regulated when yeast cells (auxotrophic for His, Lys, Leu, and Trp) were transferred, for 24 hours, to synthetic media lacking His or Lys (Fig. 4E). By contrast, starvation for Leu alone or Trp alone did not produce a similar effect (Fig. 4E). Furthermore, decreases of His in the medium could incrementally up-regulate Nt-formylated fMD-D2-GST, in contrast to similar decreases of Trp, which did not alter the (initially low) level of fMD-D2-GST (Fig. 4, F and G). Nt-formylated fMD-D2-GST was up-regulated upon starvation for His (in yeast that expressed either wild-type *Sc*Fmt1 or the cytosol-localized *Sc*Fmt1$^{\Delta 1-26}$) even in *PSH1* cells, which contained the fMet/N-end rule pathway and could degrade Nt-formylated proteins (Fig. 4, H and I).

Up-regulation of Nt-formylated fMD-D2-GST in stationary-phase cells or upon starvation for His was completely abolished in *gcn2*Δ cells, which lacked Gcn2, a stress-activated multi-functional protein kinase (Fig. 4, J and K). Even the much stronger increase, at stationary phase, of Nt-formylated fMD-D2-GST in *psh1*Δ cells (which could not destroy Nt-formylated proteins) was completely abolished in double-mutant *gcn2*Δ *psh1*Δ cells that lacked both Psh1 and Gcn2 (Fig. 4J).

Further analyses of the Gcn2 effect (Fig. 4, J and K) used Phos-tag, a phosphate-binding compound that can be linked to polyacrylamide and thereby selectively "gel shift" phosphorylated proteins, relative to their unphosphorylated (or less phosphorylated) counterparts. Phosphorylation of *Sc*Fmt1$_{myc}$ (*Sc*Fmt1 bearing a C-terminal myc tag) was substantially increased upon starvation for His in wild-type cells but did not increase in *gcn2*Δ cells (fig. S10B). Thus, large increases of Nt-formylation in the yeast cytosol upon specific starvation stresses involved the Gcn2-mediated phosphorylation of *Sc*Fmt1, a modification that may also regulate the enzymatic activity of *Sc*Fmt1 and/or its cytosolic localization, as described below.

Starvation increases the Gcn2-dependent cytosolic localization of *Sc*Fmt1

Localization of *Sc*Fmt1 was analyzed using cells expressing, from a low-copy plasmid and the native P_{FMT1} promoter, either "wild-type" *Sc*Fmt1-EGFP$_3$ (bearing three C-terminal EGFP moieties) or *Sc*Fmt1$^{\Delta 1-26}$-EGFP$_3$ (lacking the mitochondrial presequence). The *Sc*Fmt1-EGFP$_3$ fusion was functionally active and was able to rescue the impaired growth of *fmt1*Δ W303 *S. cerevisiae* on 2% glycerol–containing nonfermentable respiratory medium (fig. S10A). As would be expected, in exponentially growing cells [absorbance at 600 nm (A_{600}) < 0.8)], the bulk (> 97%) of *Sc*Fmt1-EGFP$_3$ was present in mitochondria, whereas the presequence-lacking *Sc*Fmt1$^{\Delta 1-26}$-EGFP$_3$ was distributed throughout the cytosol (Fig. 4C and fig. S10C). However, in stationary-phase cells, ~35% of wild-type *Sc*Fmt1-EGFP$_3$ became localized in the cytosol, instead of mitochondria, whereas the largely cytosolic localization of the *Sc*Fmt1$^{\Delta 1-26}$-EGFP$_3$ remained unchanged (Fig. 4, C and D, and fig. S10C).

In contrast to *Sc*Fmt1, other examined mitochondrial matrix proteins, such as Sod2, Ifm1, or Cit1, which are also translocated into the matrix from the cytosol, continued to be efficiently (>90%) imported into mitochondria even in stationary phase (fig. S11). Most tellingly, and in agreement with the above Gcn2-*Sc*Fmt1 results, the partitioning of ~35% of *Sc*Fmt1 into the cytosol in stationary-phase cells was nearly completely abrogated in *gcn2*Δ cells (Fig. 4C and fig. S10C).

Toxicity of deformylation is augmented by low temperature and azide

What might be a biological role(s) of cytosolic Nt-formylated proteins that are produced in wild-type *S. cerevisiae* and are destroyed by the fMet/N-end rule pathway? To address this question, we asked whether ectopic expression of *Ec*PDF, and the resulting deformylation of Nt-formylated proteins, might increase the sensitivity of cells to specific stressors. (Wild-type *S. cerevisiae* lacks a deformylase.) As described above, the ectopic Nt-formylation of

yeast proteins, through expression of *Ec*FMT, caused degradation of these proteins by the Psh1-mediated fMet/N-end rule pathway, including degradation of the endogenous (nonreporter) proteins Pgd1 and Rps22a (fig. S6, C to H).

The same degradation assays but with wild-type yeast (i.e., with cells that lacked ectopic *Ec*FMT and contained solely the endogenous *Sc*Fmt1) showed that the endogenous Pgd1 and Rps22a proteins became short-lived in stationary phase, a setting that strongly augments Nt-formylation (Fig. 5, A and B). The stationary-phase degradation of Pgd1 and Rps22a required Nt-formylation of these proteins because this degradation could be abolished by ectopically expressed *Ec*PDF but not by its catalytically inactive mutant *Ec*PDF^{E134A} (Fig. 5, A and B).

Furthermore, the Nt-formylation-dependent degradation of Pgd1 and Rps22a (Fig. 5, A and B) was observed only if yeast were preincubated, as streaked-out cultures on plates, for ~14 days at 4°C before inoculating cells into synthetic complete (SC) liquid medium for stationary-phase degradation assays at 30°C. A shorter, 7-day pre-incubation of yeast at 4°C did not suffice for the degradation of Pgd1 and Rps22a to take place. In agreement with these (technically robust) findings, ectopic expression of *Ec*PDF, but not of its inactive mutant, reproducibly prolonged the lag period (before exponential growth) of wild-type yeast in SC liquid medium. This effect only took place if cell growth was measured with yeast that had been preincubated at 4°C for 14 days (as described above) before their transfers to liquid cultures for growth assays (Fig. 5D). By contrast, no *Ec*PDF-mediated growth retardation was observed with cells that had not been preincubated at 4°C or were preincubated at 4°C for only 7 days (Fig. 5C and fig. S12A).

Furthermore, the expression of *Ec*PDF (but not of its inactive mutant) in cold-primed yeast (preincubated on plates at 4°C for 14 days) rendered cell growth on a galactose-containing minimal solid medium markedly hypersensitive to Na-azide, which inhibits cytochrome c oxidase, adenosine triphosphate (ATP) synthesis, and plasma membrane permeability. The same *Ec*PDF expression, under the same conditions, did not affect cell growth in the presence of other respiratory-chain inhibitors, such as antimycin A, oligomycin, or cyanide (Fig. 5E and fig. S12B). In addition, *Ec*PDF did not discernibly affect the growth of mitochondrial respiratory chain mutants *cox5a*Δ, *coq5*Δ, and *atp11*Δ (fig. S12C).

Together, these findings made it unlikely that the observed toxicity of ectopic cytosolic *Ec*PDF (its inactive mutant was nontoxic) stemmed from deformylation of the eight Nt-formylated mitochondrial matrix proteins that are encoded by mitochondrial DNA in the matrix (see introduction). The robust and reproducible dependence of the toxicity of deformylation by *Ec*PDF on a sufficiently long (~14 days) preexposure of cells to 4°C suggests that natural Nt-formylation of cytosolic eukaryotic proteins may be functionally important and potentially beneficial under conditions of specific undernutrition and/or low temperatures. Future studies will analyze this temperature effect. In nontropical climes, ecological niches of *S. cerevisiae* would sometimes expose yeast to temperatures near 0°C. Because it is likely (but remains to be verified) that Nt-formylation of cytosolic proteins is universal among eukaryotes, it would also be interesting to explore Nt-formylation in hibernating animals, whose body temperatures can become low in winter.

Our findings indicate that the observed retention of the (normally mitochondrial) *Sc*Fmt1 formyltransferase in the cytosol of stationary-phase and other starving cells is the cause of massive increases of Nt-formylated proteins. As described above, the retention of *Sc*Fmt1 in the cytosol strictly requires the Gcn2 kinase (Fig. 4, C and D, and fig. S10C). This effect of Gcn2 is apparently specific for *Sc*Fmt1, because other examined nuclear DNA–encoded mitochondrial-matrix proteins were imported into mitochondria of stationary-phase cells, despite the presence of Gcn2 (fig. S11). The observed up-regulation of Nt-formylated proteins under the above conditions may contribute, in ways that remain to be understood, to adaptations of cells to specific undernutrition stresses.

The eukaryotic fMet/N-end rule pathway

We discovered that the Nt-formylation of proteins, a long-known pretranslational protein modification previously thought to be confined to bacteria and bacteria-descended eukaryotic organelles, can also occur at the start of translation by the cytosolic ribosomes of a eukaryote such as S. *cerevisiae* (Fig. 5F). The Nt-formylation of cytosolic proteins was strongly up-regulated upon specific starvation stresses, including stationary phase or depletion of some amino acids, such as His or Lys (Fig. 4). Intriguingly, down-regulation of cytosolic Nt-formylation (through ectopic expression of deformylase) increased sensitivity of cells to specific undernutrition stresses, and/or to a prolonged cold (4°C) stress, and to Na-azide (Fig. 5 and fig. S12).

We also discovered that Nt-formylated cytosolic proteins are targeted by the Psh1 E3 Ub ligase (together with the Ubc3 E2 enzyme), which acts as the recognition component of the previously unknown eukaryotic fMet/N-end rule pathway that destroys Nt-formylated proteins (Fig. 5F). In agreement with these results, we also showed that the Psh1 fMet/N-recognin physically binds to the formyl group of the Nt-fMet residue (Fig. 3B). Nt-formylation of yeast cytosolic proteins is caused by the endogenous *Sc*Fmt1, whose translocation from the cytosol to the inner matrix of mitochondria is not as efficient, even under normal conditions, as had previously been assumed, and was strongly impaired in stationary phase (Fig. 4, C and D, and figs. S10C and S11).

We also discovered that the up-regulation of Nt-formylated cytosolic proteins in starving cells strictly requires Gcn2, a stress-activated protein kinase (Fig. 4, J and K). Gcn2 mediated the stress-induced increase of Nt-formylated proteins by controlling the cytosolic localization of the *Sc*Fmt1 enzyme and by being essential for *Sc*Fmt1 phosphorylation (Fig. 4, C and D, and fig. S10, B and C). The latter result suggests that Gcn2 may also regulate the enzymatic activity of *Sc*Fmt1.

Notably, the ability of Gcn2 to retain a large fraction of *Sc*Fmt1 in the cytosol of nutritionally stressed cells is apparently confined to *Sc*Fmt1, inasmuch as Gcn2 does not have such an effect, under the same conditions, on other examined nuclear DNA–encoded mitochondrial matrix proteins (Figs. 4C and 5F, and figs. S10C and S11). The regulation of *Sc*Fmt1 by Gcn2 is a specific protein localization circuit.

Nt-formylation and Nt-acetylation, two mutually exclusive Nt-modifications of proteins, generate, respectively, fMet/N-degrons and Ac/N-degrons (fig. S1, B and F). fMet/N-degrons are recognized by the Psh1 fMet/N-recognin, a component of the fMet/N-end rule pathway (fig. S1B). The pretranslational Nt-formylation of Met-tRNAi, by an FMT enzyme such as *Sc*Fmt1, requires 10-formyltetrahydrofolate as a cosubstrate, whereas the cotranslational Nt-acetylation of proteins by Nt-acetylases requires the acetyl coenzyme A (Ac-CoA) cosubstrate (Fig. 2A and fig. S1, B and F).

What might be an adaptive (fitness-increasing) value of the Gcn2 kinase–dependent up-regulation of Nt-formylated proteins? One possibility is that specific physiological perturbations, such as some nutritional and/or low-temperature stresses (see above), may retain adequate levels of intra-cellular 10-formyltetrahydrofolate (required for Nt-formylation) while not retaining adequate levels of Ac-CoA (required for Nt-acetylation). Under such conditions, an increased Nt-formylation of newly made proteins (through a cytosolic retention of formyltransferase) would maintain, owing to the fMet/N-end rule pathway, degradation-based protein quality control. As shown previously, in the absence of stress, this control is mediated, in part, by the Ac/N-end rule pathway (9–13). In the resulting model, the fMet/N-end rule pathway and the Ac/N-end rule pathway are functionally complementary, in that the former may assist the latter under metabolic conditions that favor Nt-formylation over Nt-acetylation. The fMet/N-end rule pathway (fig. S1, A and B) is the fourth eukaryotic N-end rule pathway that was discovered over the past three decades. The three previously identified N-end rule pathways are universal among eukaryotes (fig. S1, E to G) (9–15, 20). The fMet/N-end rule pathway (Fig. 5F and fig. S1B) is likely to be universal as well, given strongly conserved mechanisms that mediate Nt-formylation and degron recognition.

Materials and methods summary

Yeast strains, plasmids, genetic techniques, and degradation assays

Standard techniques were used for construction of plasmids and strains. Protein degradation as-says were performed largely as described (9, 11). Tables S3 to S5 list *S. cerevisiae* strains, plasmids, and PCR primers. See supplementary materials and methods for details.

Mass spectrometric analyses

SILAC and cLC-MS/MS were carried out as described in the supplementary materials and methods.

Production of antibodies specific for two Nt-formylated proteins

Nt-formylated peptides and its unformylated counterparts were synthesized by Abfrontier or AbClon (Seoul, Republic of Korea). Production and purification of anti–MD-D2^{fM} and anti-Cse4^{fM} antibodies (Fig. 1, D to G, and fig. S4, C and D) are described in the supplementary materials and methods.

GST-pulldown assays with Psh1

Nt-formylated fMD-D2-GST and its unformylated MD-D2-GST counterpart were produced using *E. coli* in either the presence or absence of actinonin, a deformylase inhibitor. GST-pulldowns with yeast extracts containing C-terminally flag-tagged *S. cerevisiae* Psh1 ($Psh1_f$) used purified Nt-formylated fMD-D2-GST versus unformylated MD-D2-GST and were carried out as described in the supplementary materials and methods.

Supplementary Material

Refer to Web version on PubMed Central for supplementary material.

ACKNOWLEDGMENTS

We thank W.-K. Huh (Seoul National University, Seoul, Republic of Korea) for yeast deletion library mutants, S. Biggins (Hutchinson Cancer Center, Seattle, WA, USA) for pSB1535 and pSB1541, and R. Sauer (MIT, Cambridge, MA, USA)for AG110A(DE) *E. coli*. We also thank the present and former members of the Hwang laboratory for their assistance and advice.

Funding:

This work was supported by grants from the Samsung Science & Technology Foundation (SSTF-BA1401–17) and the BK21 plus program (C.-S.H.), by NRF grants of the Korean Government (MSIP) [NRF-2017M3A9F9030559 (C.L.) and NRF-2017R1A5A1015366 (J.-Y.Y.)], and by NIH grants R01GM031530 and R01DK039520 (A.V.).

REFERENCES AND NOTES

1. Laursen BS, Sørensen HP, Mortensen KK,Sperling-Petersen HU, Initiation of protein synthesis in bacteria. Microbiol. Mol. Biol. Rev 69, 101–123 (2005). doi: 10.1128/MMBR.69.1.101-123.2005; [PubMed: 15755955]
2. Mazel D, Pochet S, Marlière P, Genetic characterization of polypeptide deformylase, a distinctive enzyme of eubacterial translation. EMBO J. 13, 914–923 (1994). doi: 10.1002/j.1460-2075.1994.tb06335.x; [PubMed: 8112305]
3. Kramer G, Boehringer D, Ban N, Bukau B, The ribosome as a platform for co-translational processing, folding and targeting of newly synthesized proteins. Nat. Struct. Mol. Biol 16, 589–597 (2009). doi: 10.1038/nsmb.1614; [PubMed: 19491936]
4. Ramesh V, Köhrer C, RajBhandary UL, Expression of *Escherichia coli* methionyl-tRNA formyltransferase in *Saccharomyces cerevisiae* leads to formylation of the cytoplasmic initiator tRNA and possibly to initiation of protein synthesis with formylmethionine. Mol. Cell. Biol 22, 5434–5442 (2002). doi: 10.1128/MCB.22.15.5434-5442.2002; [PubMed: 12101237]
5. Bingel-Erlenmeyer R et al., A peptide deformylase-ribosome complex reveals mechanism of nascent chain processing. Nature 452, 108–111 (2008). doi: 10.1038/nature06683; [PubMed: 18288106]
6. Giglione C, Fieulaine S, Meinnel T, N-terminal protein modifications: Bringing back into play the ribosome. Biochimie 114, 134–146 (2015). doi: 10.1016/j.biochi.2014.11.008; [PubMed: 25450248]
7. Piatkov KI, Vu TTMH, Hwang C-S, Varshavsky A, Formyl-methionine as a degradation signal at the N-termini of bacterial proteins. Microb. Cell 2, 376–393 (2015).doi: 10.15698/mic2015.10.231; [PubMed: 26866044]
8. Aksnes H, Drazic A, Marie M, Arnesen T, First things first: Vital protein marks by N-terminal acetyltransferases. Trends Biochem. Sci 41, 746–760 (2016). doi: 10.1016/j.tibs.2016.07.005; [PubMed: 27498224]
9. Hwang CS, Shemorry A, Varshavsky A, N-terminal acetylation of cellular proteins creates specific degradation signals. Science 327, 973–977 (2010). doi: 10.1126/science.1183147; [PubMed: 20110468]

10. Varshavsky A, The N-end rule pathway and regulation by proteolysis. Protein Sci. 20, 1298–1345 (2011). doi: 10.1002/pro.666; [PubMed: 21633985]
11. Shemorry A, Hwang CS, Varshavsky A, Control of protein quality and stoichiometries by N-terminal acetylation and the N-end rule pathway. Mol. Cell 50, 540–551 (2013).doi: 10.1016/j.molcel.2013.03.018; [PubMed: 23603116]
12. Kim HK et al., The N-terminal methionine of cellular proteins as a degradation signal. Cell 156, 158–169 (2014). doi: 10.1016/j.cell.2013.11.031; [PubMed: 24361105]
13. Park SE et al., Control of mammalian G protein signaling by N-terminal acetylation and the N-end rule pathway. Science 347, 1249–1252 (2015). doi: 10.1126/science.aaa3844; [PubMed: 25766235]
14. Bachmair A, Finley D, Varshavsky A, In vivo half-life of a protein is a function of its amino-terminal residue. Science 234, 179–186 (1986). doi: 10.1126/science.3018930; [PubMed: 3018930]
15. Tasaki T, Sriram SM, Park KS, Kwon YT, The N-end rule pathway. Annu. Rev. Biochem 81, 261–289 (2012).doi: 10.1146/annurev-biochem-051710-093308; [PubMed: 22524314]
16. Finley D, Ulrich HD, Sommer T, Kaiser P, The ubiquitin-proteasome system of *Saccharomyces cerevisiae*. Genetics 192, 319–360 (2012). doi: 10.1534/genetics.112.140467; [PubMed: 23028185]
17. Schmidt R, Zahn R, Bukau B, Mogk A, ClpS is the recognition component for *Escherichia coli* substratesof the N-end rule degradation pathway. Mol. Microbiol 72, 506–517 (2009). doi: 10.1111/j.1365-2958.2009.06666.x; [PubMed: 19317833]
18. Gibbs DJ, Bacardit J, Bachmair A, Holdsworth MJ, The eukaryotic N-end rule pathway: Conserved mechanisms and diverse functions. Trends Cell Biol. 24, 603–611 (2014). doi: 10.1016/j.tcb.2014.05.001; [PubMed: 24874449]
19. Dissmeyer N, Rivas S, Graciet E, Life and death of proteins after protease cleavage: Protein degradation by the N-end rule pathway. New Phytol. 218, 929–935 (2018). doi: 10.1111/nph.14619; [PubMed: 28581033]
20. Chen SJ, Wu X, Wadas B, Oh J-H, Varshavsky A, An N-end rule pathway that recognizes proline and destroys gluconeogenic enzymes. Science 355, eaal3655 (2017).doi: 10.1126/science.aal3655; [PubMed: 28126757]
21. Rivera-Rivera I, Román-Hernández G, Sauer RT, Baker TA, Remodeling of a delivery complex allows ClpS-mediated degradation of N-degron substrates. Proc. Natl. Acad. Sci. U.S.A. 111, E3853–E3859 (2014). doi: 10.1073/pnas.1414933111; [PubMed: 25187555]
22. Shim SM et al., The endoplasmic reticulum-residing chaperone BiP is short-lived and metabolized through N-terminal arginylation. Sci. Signal 11, eaan0630 (2018). doi: 10.1126/scisignal.aan0630; [PubMed: 29295953]
23. Oh JH, Hyun JY, Varshavsky A, Control of Hsp90 chaperone and its clients by N-terminal acetylation and the N-end rule pathway. Proc. Natl. Acad. Sci. U.S.A 114, E4370–E4379 (2017). doi: 10.1073/pnas.1705898114; [PubMed: 28515311]
24. Piatkov KI, Brower CS, Varshavsky A, The N-end rule pathway counteracts cell death by destroying proapoptotic protein fragments. Proc. Natl. Acad. Sci. U.S.A 109, E1839–E1847 (2012). doi: 10.1073/pnas.1207786109; [PubMed: 22670058]
25. Wadas B, Piatkov KI, Brower CS, Varshavsky A, Analyzing N-terminal arginylation through the use of peptide arrays and degradation assays. J. Biol. Chem 291, 20976–20992 (2016). doi: 10.1074/jbc.M116.747956; [PubMed: 27510035]
26. Hu R-G et al., The N-end rule pathway as a nitric oxide sensor controlling the levels of multiple regulators. Nature 437, 981–986 (2005). doi: 10.1038/nature04027; [PubMed: 16222293]
27. Scott DC, Monda JK, Bennett EJ, Harper JW,Schulman BA, N-terminal acetylation acts as an avidity enhancer within an interconnected multiprotein complex. Science 334, 674–678 (2011). doi: 10.1126/science.1209307; [PubMed: 21940857]
28. Hwang C-S, Shemorry A, Auerbach D, Varshavsky A, The N-end rule pathway is mediated by a complex of the RING-type Ubr1 and HECT-type Ufd4 ubiquitin ligases. Nat. Cell Biol. 12, 1177–1185 (2010). doi: 10.1038/ncb2121; [PubMed: 21076411]

29. Choi WS et al., Structural basis for the recognition of N-end rule substrates by the UBR box of ubiquitin ligases. Nat. Struct. Mol. Biol 17, 1175–1181 (2010). doi: 10.1038/nsmb.1907; [PubMed: 20835240]

30. Matta-Camacho E, Kozlov G, Li FF, Gehring K, Structural basis of substrate recognition and specificity in the N-end rule pathway. Nat. Struct. Mol. Biol 17, 1182–1187 (2010).doi: 10.1038/nsmb.1894; [PubMed: 20835242]

31. Kim MK, Oh SJ, Lee BG, Song HK, Structural basis for dual specificity of yeast N-terminal amidase in the N-end rule pathway. Proc. Natl. Acad. Sci. U.S.A. 113, 12438–12443 (2016). doi: 10.1073/pnas.1612620113; [PubMed: 27791147]

32. Varshavsky A, 'Spalog' and 'sequelog': Neutral terms for spatial and sequence similarity. Curr. Biol 14, R181–R183 (2004). doi: 10.1016/j.cub.2004.02.014; [PubMed: 15028230]

33. Hewawasam G et al., Psh1 is an E3 ubiquitin ligase that targets the centromeric histone variant Cse4. Mol. Cell 40, 444–454 (2010). doi: 10.1016/j.molcel.2010.10.014; [PubMed: 21070970]

34. Ranjitkar P et al., An E3 ubiquitin ligase prevents ectopic localization of the centromeric histone H3 variant via the centromere targeting domain. Mol. Cell 40, 455–464 (2010). doi: 10.1016/j.molcel.2010.09.025; [PubMed: 21070971]

35. Au WC et al., A novel role of the N terminus of budding yeast histone H3 variant Cse4 in ubiquitin-mediated proteolysis. Genetics 194, 513–518 (2013). doi: 10.1534/genetics.113.149898; [PubMed: 23525333]

36. Metzger MB, Scales JL, Dunklebarger MF, Weissman AM, The ubiquitin ligase (E3) Psh1p is required for proper segregation of both centromeric and two-micron plasmids in *Saccharomyces cerevisiae*. G3 (Bethesda) 7, 3731–3743 (2017). [PubMed: 28928274]

37. Cheng H, Bao X, Gan X, Luo S, Rao H, Multiple E3s promote the degradation of histone H3 variant Cse4. Sci. Rep 7, 8565 (2017). doi: 10.1038/s41598-017-08923-w; [PubMed: 28819127]

38. Robinson PJ et al., Structure of a complete mediator-RNA polymerase II pre-initiation complex. Cell 166, 1411–1422.e16 (2016). doi: 10.1016/j.cell.2016.08.050; [PubMed: 27610567]

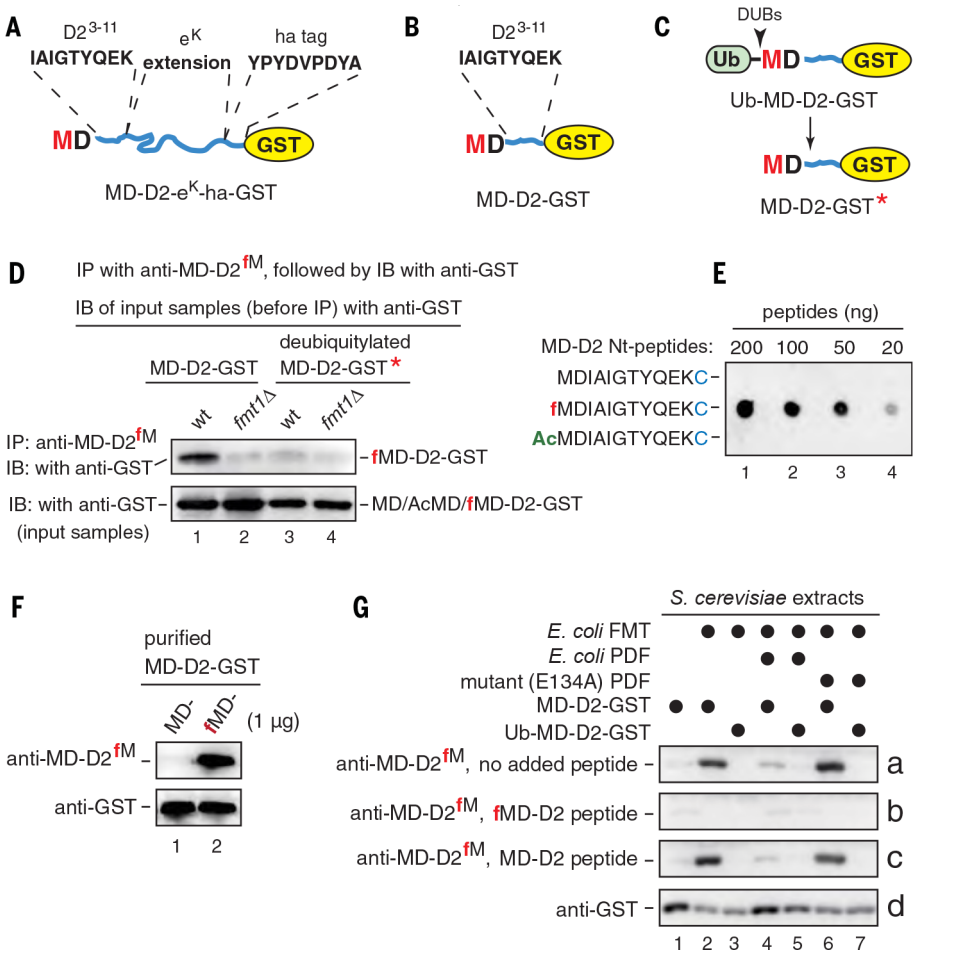

Fig. 1. Antibody specific for a set of N-terminally formylated reporters.

(A) MD-D2-e^{K}-ha-GST and some of its amino acid sequences. (**B**) MD-D2-GST, same fusion as in (A) but lacking the e^{K}-ha segment. (**C**) Same fusion as in (B) but including the Nt-Ub moiety. (**D**) fMD-D2-GSTis produced in wild-type yeast. Lane 1, upper panel: MD-D2-GST was expressed in wild-type (*FMT1*) *S. cerevisiae* and was immunoprecipitated (IP) from yeast extracts with anti–MD-D2^{fM} antibody (which selectively recognized Nt-formylated fMD-D2-GST), followed by SDS-PAGE and immunoblotting (IB) with anti-GST. Lane 2: Same as lane 1 but with *fmt1*Δ yeast. Lane 3: Same as lane 1 but with Ub-MD-D2-GST. Lane 4: Same as lane 3 but with *fmt1*Δ yeast. Lower panel, inputs: Immunoblotting with anti-GST. The red asterisk in (C) and (D) indicates a version of the MD-D2-GST fusion that was produced through deubiquitylation of Ub-MD-D2-GST. (**E**) Dot immunoblotting with anti–MD-D2^{fM} antibody versus decreasing amounts of the unmodified MDIAIGTYQEKC peptide and either its Nt-formylated or its Nt-acetylated counterparts. (**F**) Purified unformylated MD-D2-GST (lane 1) and Nt-formylated fMD-D2-GST (lane 2) were subjected to SDS-PAGE and immunoblotting with either anti–MD-D2^{fM} (upper panel) or anti-GST (lower panel). (**G**) Pretranslational Nt-formylation of MD-D2-GST. The upper three panels show immunoblots, using anti–MD-D2^{fM}, of SDS-PAGE-fractionated extracts from *S. cerevisiae* that expressed (or did not express) specific proteins indicated above the panels (see the main text). Immunoblots a, b, and c with anti–MD-D2^{fM} were performed in

the absence or presence of the indicated peptides. Immunoblot d is the same as immunoblot a but with anti-GST.

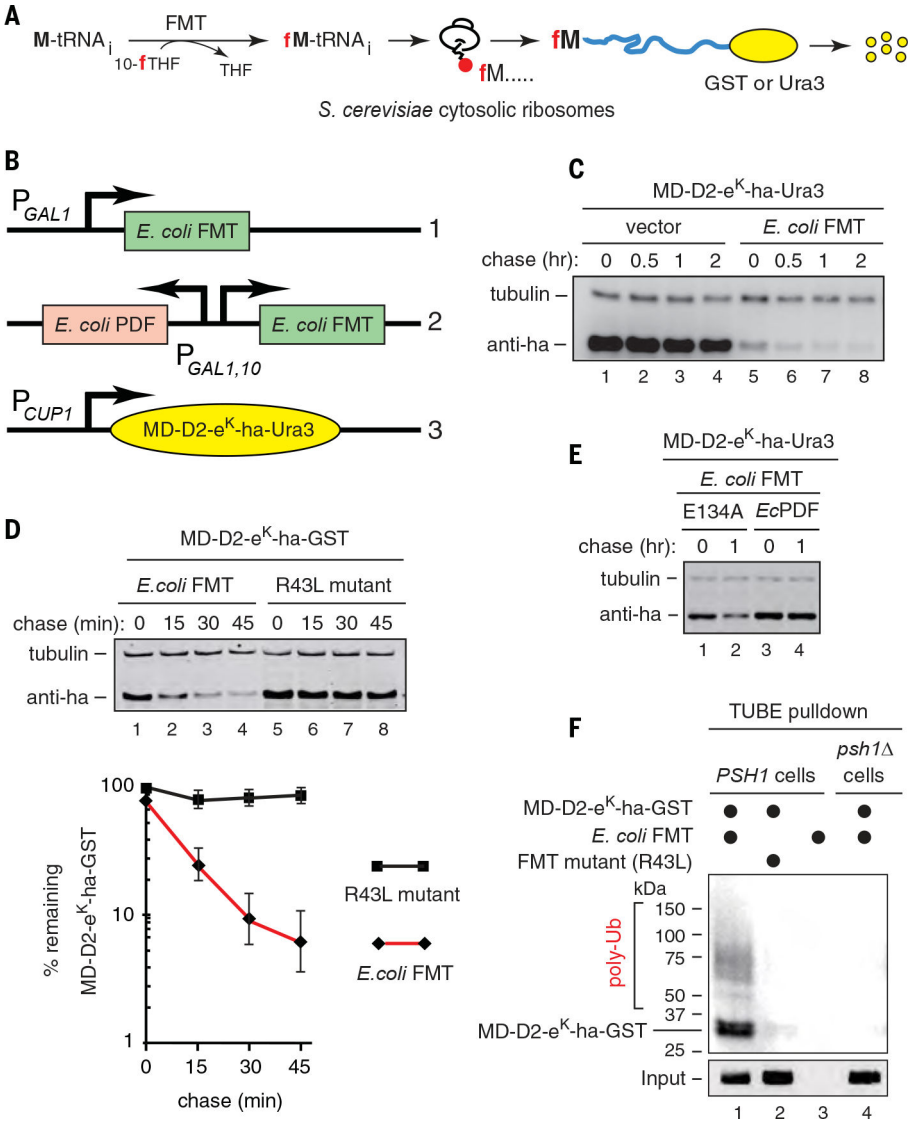

Fig. 2. Selective in vivo degradation of Nt-formylated proteins.

(**A**) A diagram of the fMet-mediated cytosolic synthesis and degradation of a GST-based or Ura3-based Nt-formylation reporter (relevant to Figs. 2, B to F, and 3A, and to figs. S4, E to I). tRNAi, initiator transfer RNA. (**B**) Diagrams for the expression of *Ec*FMT, *Ec*PDF, or MD-D2-e^K-ha-Ura3. 1) A high-copy plasmid expressing *Ec*FMT in *S. cerevisiae* from the P$_{GAL1}$ promoter, 2) a high-copy plasmid expressing *Ec*FMT and *Ec*PDF from the bidirectional P$_{GAL1,10}$ promoter, and 3) a low-copy plasmid expressing MD-D2-e^K-ha-Ura3 (or MD-D2-e^K-ha-GST) from the P$_{CUP1}$ promoter. (**C**) CHX-chases with MD-D2-e^K-ha-Ura3 in *naa20*Δ *ubr1*Δ *S. cerevisiae* (see the main text) that expressed either vector alone (lanes 1 to 4) or *Ec*FMT (lanes 5 to 8). Immunoblotting was performed with anti-ha. (**D**) Same as in (C) but with MD-D2-e^K-ha-GST and cells that expressed either *Ec*FMT (lanes 1 to 4) or its inactive *Ec*FMT^{R43L} mutant (lanes 5 to 8). The graph shows quantification of data (three independent pairs of CHX-chases), with mean ± standard error. (**E**) CHX-chases, using anti-ha, with MD-D2-e^K-ha-Ura3 in *naa20*Δ *ubr1*Δ *S. cerevisiae* that expressed wild-

type *Ec*FMT and also expressed either wild-type *Ec*PDF (lanes 3 and 4) or its inactive *Ec*PDF^{E134A} mutant (lanes 1 and 2). (**F**) TUBE-pulldowns with *S. cerevisiae* expressing (or not expressing) either MD-D2-e^{K}-ha-GST or *Ec*FMT or its *Ec*FMT^{R43L} mutant, with anti-GST immunoblotting, after TUBE-pulldowns. The lower panel shows inputs and immunoblotting with anti-GST.

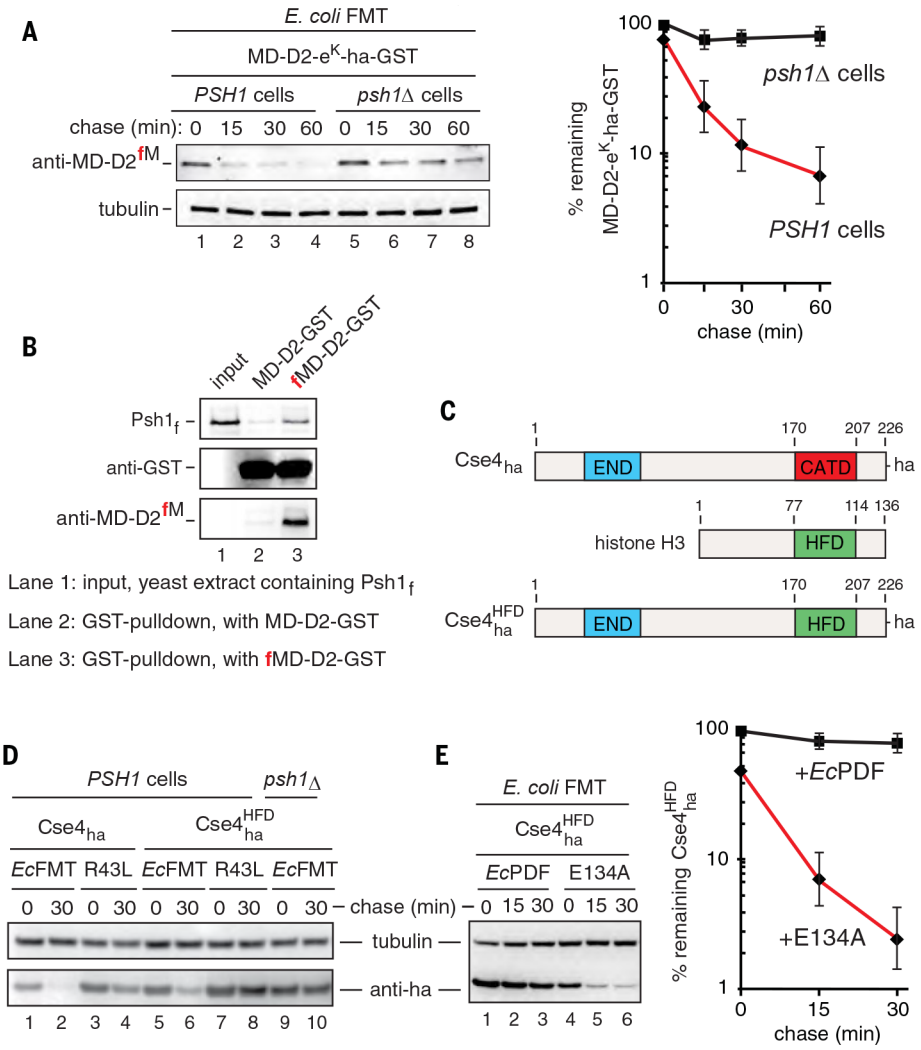

Fig. 3. The Psh1 E3 Ub ligase as an fMet/N-recognin.

(**A**) CHX-chases with MD-D2-e^{K}-ha-GST in *naa20*Δ *ubr1*Δ *S. cerevisiae* (see the main text) that expressed *Ec*FMT and either contained (lanes 1 to 4) or lacked (lanes 5 to 8) the Psh1 E3. Immunoblotting with anti–fMD-D2^{fM}. The graph shows quantification of data (three independent pairs of CHX-chases), with mean ± standard error. (**B**) GST-pulldowns with purified Nt-formylated fMD-D2-GST versus unformylated MD-D2-GST and extracts of *S. cerevisiae* that expressed Psh1$_{f}$ (see materials and methods). Detection with anti-flag (specific for Psh1$_{f}$), anti-GST, and anti–fMD-D2^{fM} (specific for Nt-formylated fMD-D2-GST). Lanes 1 to 3 are described in (B). Note specific binding of Psh1$_{f}$ to fMD-D2-GST. (**C**) Wild-type ha-tagged Cse4$_{ha}$, histone H3, and "hybrid" Cse4$^{HFD}_{ha}$ (see the main text). (**D**) CHX-chases with Cse4$_{ha}$ (lanes 1 to 4) and Cse4$^{HFD}_{ha}$ (lanes 5 to 10) in *S. cerevisiae* expressing *Ec*FMT or its *Ec*FMT^{R43L} mutant. Lanes 9 and 10 are the same as lanes 5 and 6 but in *psh1*Δ yeast. Immunoblotting was performed with anti-ha. (**E**) CHX-chases of Cse4$^{HFD}_{ha}$ in *Ec*FMT-expressing *S. cerevisiae* that also expressed *Ec*PDF (lanes 1 to 3) or its

inactive *Ec*PDF^{E134A} mutant (lanes 4 to 6). The graph shows quantification of data (three independent pairs of CHX-chases), with mean ± standard error.

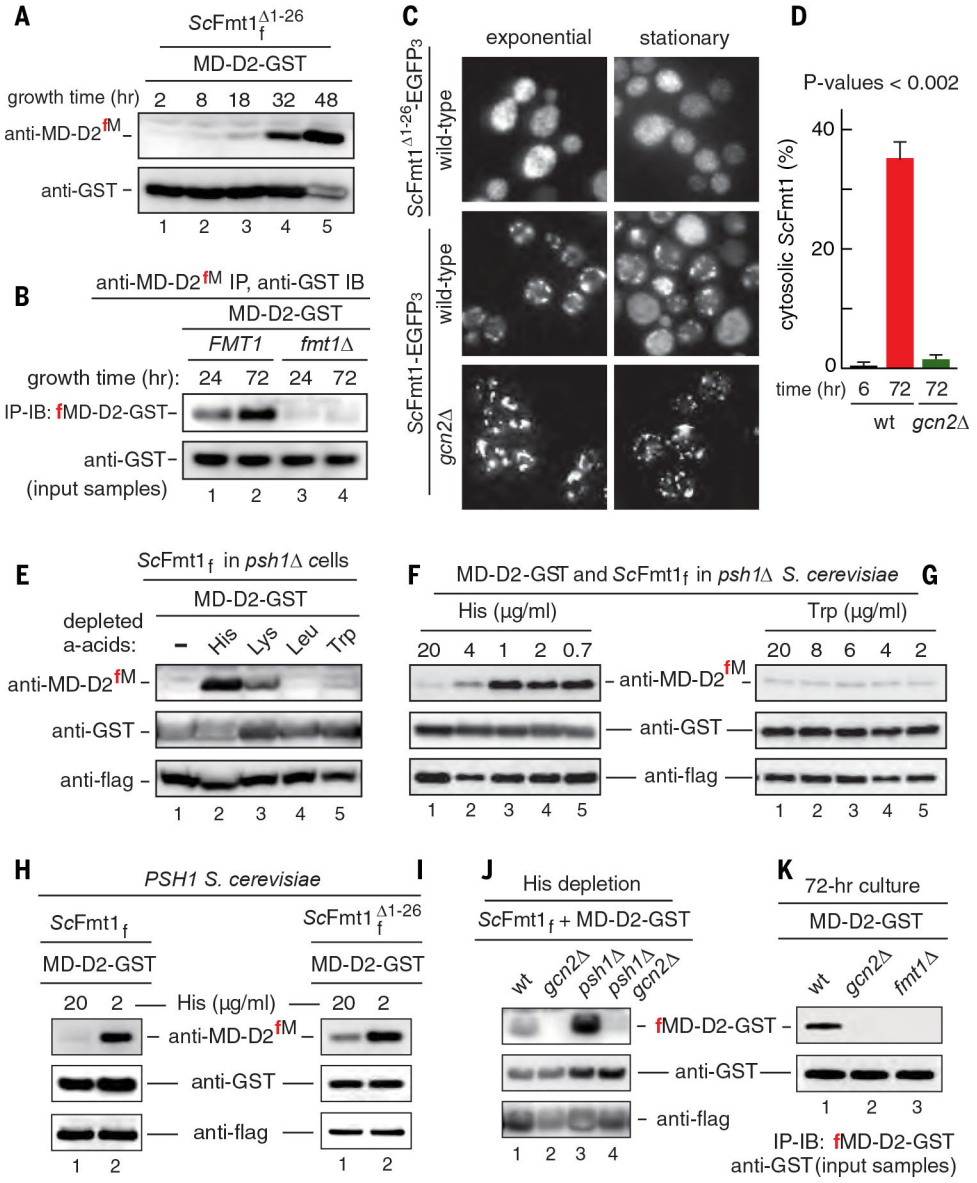

Fig. 4. Up-regulation of Nt-formylated proteins and cytosolic localization of mitochondrial formyltransferase upon starvation in yeast.

(**A**) *S. cerevisiae* expressing MD-D2-GST and the mitochondrial presequence–lacking *Sc*Fmt1 $^{\Delta 1-26}{}_{f}$ were grown in SC medium until stationary phase (48 hours), followed by SDS-PAGE of cell extracts and detection of Nt-formylated fMD-D2-GST by immunoblotting with anti–MD-D2^{fM}. The lower panel shows immunoblotting with anti-GST. (**B**) *FMT1* (lanes 1 and 2) and *Sc*Fmt1-lacking *fmt1*Δ *S. cerevisiae* (lanes 3 and 4) expressing MD-D2-GST were grown in SC medium from 24 to 72 hours (reaching stationary phase), followed by immunoprecipitation of cell extracts with anti–MD-D2^{fM}, SDS-PAGE of immunoprecipitates, and immunoblotting with anti-GST (upper panel). The lower panel shows immunoblotting with anti-GST, but of total (input) samples.(**C**) Representative images of fluorescent wild-type cells expressing, respectively, the presequence-lacking *Sc*Fmt1$^{\Delta 1-26}$-EGFP$_3$ fusion (two upper squares) and wild-type

*Sc*Fmt1-EGFP$_3$ (two middle squares). The two bottom squares show *gcn2*Δ cells expressing wild-type *Sc*Fmt1-EGFP$_3$. The left and right squares show, respectively, cells in exponential growth and in stationary phase. Note the increased cytosolic localization of *Sc*Fmt1-EGFP$_3$ in wild-type cells in stationary phase (middle-right square) but not in stationary-phase *gcn2*Δ cells (bottom-right square). (**D**) Relative amounts of the cytosolically localized *Sc*Fmt1-EGFP$_3$ in wild-type cells during exponential growth (6-hour growth) and in stationary-phase (72-hour growth) wild-type versus *gcn2*Δ cells. The data are shown as means ± standard deviations for ~300 cells in each of three independent experiments. *P* values of less than 0.002 were calculated using a two-tailed Student's *t* test. (**E**) Stationary (48 hour; A_{600} of ~3.5) cultures of *psh1*Δ *S. cerevisiae* (auxotrophic for His, Lys, Leu, and Trp) expressing MD-D2-GST and the wild-type flag-tagged *Sc*Fmt1$_f$ in SC medium were incubated for another 24 hours in fresh SC that either contained His, Lys, Leu, and Trp (lane 1) or lacked either His, Lys, Leu, or Trp (lanes 2 to 5, respectively). SDS-PAGE of cell extracts was followed by immunoblotting with anti–MD-D2^{fM}, anti-GST, and anti-flag. a-acids, amino acids.(**F**) Twenty-four–hour cultures (A_{600} of ~3.0) of *psh1*Δ *S. cerevisiae* (auxotrophic for His, Lys, Leu, and Trp) expressing MD-D2-GST and wild-type *Sc*Fmt1$_f$ were diluted to A_{600} of ~0.1 and thereafter were grown for 48 hours in SC that contained either the standard (20 μg/ml) concentration of His (lane 1) or decreasing concentrations of His, as indicated in lanes 2 to 5, followed by immunoblotting as described in (E). (**G**) Same as in (F) but with Trp instead of His. (**H** and **I**) Twenty-four–hour cultures (A_{600} of ~3.0) of *PSH1 S. cerevisiae* expressing MD-D2-GST and either wild-type *Sc*Fmt1$_f$ (H) or *Sc*Fmt1$_f$ $^{\Delta 1–26}$ (I) were diluted to A_{600} of ~0.1 and thereafter were grown for 48 hours in SC containing His at either 20 or2 μg/ml, followed by SDS-PAGE of cell extracts and immunoblotting with anti–MD-D2^{fM}, anti-GST, and anti-flag. (**J**) *S. cerevisiae* (A_{600} of ~3.5), of the indicated genotypes, expressing MD-D2-GST and wild-type *Sc*Fmt1$_f$, were incubated for another 24 hours in the absence of added His, followed by analyses described in (E). (**K**) Wild-type, *gcn2*Δ, and *fmt1*Δ *S. cerevisiae* expressing MD-D2-GST were grown in SC to stationary phase (for 72 hours) and were analyzed by immunoblotting, as in (B).

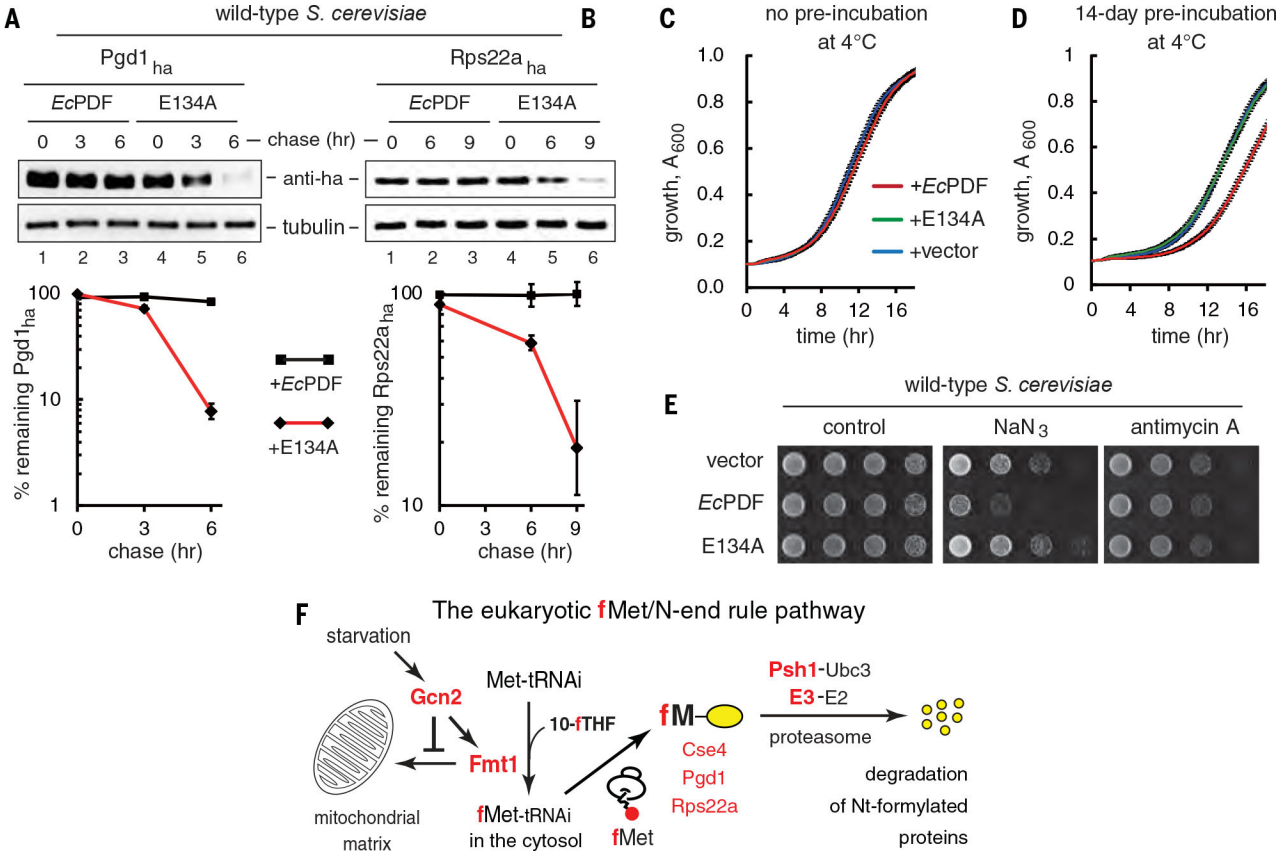

Fig. 5. Toxicity of deformylase is augmented by low temperature and azide.

(**A**) CHX-chases for 0, 3, and 6 hours with C-terminally ha-tagged $Pgd1_{ha}$ and 48-hour culture (stationary phase) of wild-type *S. cerevisiae* that expressed either *Ec*PDF or its catalytically inactive *Ec*PDF^{E134A} mutant. Before these assays in liquid cultures, cells were kept as streaked-out cultures on plates for ~14 days at 4°C (see the main text). The graphs show quantification of data (three independent pairs of CHX-chases), with mean ± standard error. (**B**) Same as in (A), but CHX-chases were for 0, 6, and 9 hours with $Rps22a_{ha}$. (**C**) Growth (A_{600}) of wild-type yeast in SC medium, measured in 96-well microplates using orbital shaker and Epoch 2 microplate spectrophotometer. *S. cerevisiae* expressed either vector alone or *Ec*PDF or its inactive *Ec*PDF^{E134A} mutant and were not preincubated at 4°C. Note indistinguishable rates of growth, irrespective of expression of *Ec*PDF. (**D**) Same as in (C) but yeast were kept as streaked-out cultures on plates for 14 days at 4°C [see (A) and the main text] before growth assays in liquid culture. Note a discernibly slower growth, with preincubation at 4°C, of cells that expressed *Ec*PDF (but not its inactive *Ec*PDF^{E134A} mutant). In (C) and (D), each point on the curve also shows ± standard error of A_{600} values (at 10-min intervals), with measurements carried out independently six times. (**E**) Wild-type *S. cerevisiae* that expressed either vector alone or *Ec*PDF or its inactive *Ec*PDF^{E134A} mutant were serially diluted (fivefold) and spotted on galactose-containing minimal medium (SGal) plates with or without either 20 μM NaN_3 or 20 nM antimycin A. The plates were incubated at 30°C for 3 days. As in (A) to (D), yeast cells were kept for ~14 days at 4°C before 16-hour liquid-culture growth and spot assays. (**F**) A partial summary of main results. Upon specific nutritional stresses (including stationary phase), the *Sc*Fmt1 formyltransferase is

substantially retained in the cytosol, an alteration that strictly requires the Gcn2 kinase, which phosphorylates *Sc*Fmt1 and might also increase its enzymatic activity. The effect of Gcn2 on the cytosolic retention of *Sc*Fmt1 appears to be confined to *Sc*Fmt1, that is, it does not extend to other nuclear DNA–encoded mitochondrial matrix proteins. The increased cytosolic localization of *Sc*Fmt1 increases production of cytosolic fMet-tRNAi, and thereby up-regulates cytosolic Nt-formylated proteins. The latter are targeted for degradation by the Psh1 Ub ligase, the fMet/N-recognin of the proteasome-mediated fMet/N-end rule pathway.